A MULTI-STAGE MODEL FOR DIELECTRIC BARRIER DISCHARGE IN ATMOSPHERIC PRESSURE AIR

A. Cristofolini[(1)], A. Popoli[(1)], G. Neretti[(1)]

[1]Department of Electrical, Electronic and Information Engineering « Guglielmo Marconi », University of Bologna,
Viale del Risorgimento, 2, 40136, Bologna, Italy

ABSTRACT. In this paper, a multi-stage numerical methodology for the description of the Dielectric Barrier Discharge physics in air is discussed. The behavior of the heavy species is computed using drift-diffusion equations. Electrons are taken into account by solving a non-linear formulation of electrostatics. The physical effects of the steamer discharges are modelled by means of a simplified 0D approach. The model also includes a semi-implicit 0D model for the assessment of the elementary chemical processes occurring in air. The developed methodology is employed for the simulation of a volumetric Dielectric Barrier Discharge reactor. The obtained species number density and surface charge deposition rates and are shown and discussed.

Keywords : DBD plasma, Dielectric Barrier Discharge, Plasma Modelling, Plasma Processing, Plasma Actuators

Corresponding author:
Andrea Cristofolini
Department of Electrical, Electronic and Information Engineering « Guglielmo Marconi », University of Bologna,
Viale del Risorgimento, 2, 40136, Bologna, Italy
Tel : +39 051 2093568
Fax : +39 051 2093588
Email : andrea.cristofolini@unibo.it

INTRODUCTION

A cold plasma device combines the advantages associated with the use of a plasma in a non-equilibrium regime with the convenience of operating at atmospheric pressure and with the flexibility in the choice of the materials employed. The Dielectric Barrier Discharge (DBD) is a physical phenomenon that can conveniently be used to produce a cold plasma. The industrial and technological applications of the DBD are numerous and concern the most disparate areas. Fluid dynamic actuators have been proposed and actively investigated for applications in the aeronautical [1]–[3], automotive [4], and turbomachinery fields [5]. DBDs in air usually produce several active chemical species (ozone, OH radicals, etc.), which are the basis for various applications aimed at material processing [6], gas and liquid flow treatment [7], sterilization, and combustion [8]. Despite the relative ease by which it is possible to create a DBD based device, the phenomenon involves a range of highly complex physical mechanisms. A DBD model that aims at a fine analysis of the phenomenon to acquire a deeper knowledge of the elementary processes must therefore address a wide range of difficulties.

One of the major challenges in modelling the cold plasma produced by a DBD is to adequately represent the non-equilibrium regime. Particularly, streamer dominated discharges are characterized by wide differences in time scales and characteristic lengths; from a numerical perspective, this physical feature leads to prohibitive computational burden for computer codes devoted to the modelling of such phenomena. For this reason, a multi-stage model of the discharge is proposed, extending the capabilities of the numerical method introduced in [9].

The developed methodology utilizes a drift-diffusion formulation to describe the collective behavior of the heavy particles (i.e. ions and molecules). The free electrons are assumed to instantly adapt their distribution to the electrostatic field, which is computed at each time-step by solving a nonlinear Poisson equation. As a result of this, the time-step length required to grant the numerical stability of the drift-diffusion equations is limited by the physical properties of the heavy species, rather than the electrons. In this way, the employed time step lengths are nearly three orders of

magnitude higher; this leads to great beneficial effects in terms of computational times in comparison to existing approaches based on formulations that include the electrons in the drift and diffusion equations [10]–[13]. In order account for the global effects of the streamers, a zero-dimensional simplified model, based on lumped circuital elements, is proposed. The model also includes a description of the plasma kinetics and of the chemical reactions, as well as a treatment of the discharge interactions with the dielectric.

With respect to the work in [9], here the number of chemical species (both charged and neutral) has been extended to include the ozone formation chain. Moreover, the model has been applied to a realistic physical configuration, focusing on the effects of charge deposition on the dielectric layers covering the electrodes.

PHYSICAL FORMULATION

Drift-Diffusion model

As anticipated, the model employs drift and diffusion equations to describe dynamics of the ionic species in the plasma:

$$\frac{\partial \mathrm{N_s}}{\partial \mathrm{t}} = -\nabla \cdot \left(-\mathrm{D_s}\nabla \mathrm{N_s} + \mu_\mathrm{s}\vec{\mathrm{E}}\mathrm{N_s}\right) + \Omega_\mathrm{s} + \Omega_{\mathrm{s,streamer}}. \qquad (1)$$

In (1), the fluxes of the generic heavy species N_s depend both on diffusion and charge drift caused by the electric field $\vec{E}$. $\mathrm{D_s}$ and μ_s represent the diffusion coefficient and electrical mobility of the s species, respectively. The source terms appearing in the right-hand side of (1) are attributable to two different mechanisms: Ω_s indicates the number of particles belonging to the s species produced in the unit time and volume due the chemical reactions in the diffused phase of the discharge (i.e., thermal ionizations, recombinations, attachments), while $\Omega_{s,streamer}$ represents the production processes due to the Townsend avalanche effect taking place in the streamers. In order to provide a

simplified description of an atmospheric pressure air plasma, 4 neutral species (N_2, O_2, O_3, O) and 5 charged species (N_2^+, O_2^+, O_2^-, O^-, and e^-), have been considered in the calculations. Since the present work focuses on a describing the DBD physics in the heavy particles time scale, (1) applies to all the above listed charged species except the electrons. For what concerns the 4 considered neutral species, their mobility is assumed to be zero and (1) retains only the diffusion term.

Electrostatics

Thanks to the assumption of conservative electric field, the electric potential in the discharge region is given by Poisson's equation:

$$\nabla^2\varphi = -\frac{\rho}{\epsilon_0}, \tag{2}$$

where the electric charge density ρ depends on the spatial distribution of the ions and electrons number densities. While the heavy particles are modelled through the drift diffusion equations described in the previous section, electrons, being much faster than ions, are considered to adapt instantaneously to the local value of the electric potential, according to the Boltzmann relation. Thus, a non linear expression for the Poisson's equation is obtained:

$$\nabla^2\varphi = -\frac{e}{\epsilon_0}\left[N_{N_2^+} + N_{O_2^+} - N_{O_2^-} - N_{O^-} - N_{e,0}\exp\left(\frac{\varphi-\varphi_0}{T_{e,eV}}\right)\right], \tag{3}$$

where $T_{e,eV} = k_B T_e/e$ is the electron temperature in eV, φ_0 the electric reference potential and $N_{e,0}$ the background electron number density.

As discussed in [9], none of the above relations guarantees that the total electric charge in the domain is equal to zero. Therefore, an additional constraint is added to enforce that - at each time-

step - the net charge due to the heavy species and the surface charge stored on the dielectric layers is neutralized by the total negative charge due to electrons:

$$e\int_{\mathrm{V}}\left[\mathrm{N}_{\mathrm{N}_2^+}+\mathrm{N}_{\mathrm{O}_2^+}-\mathrm{N}_{\mathrm{O}_2^-}-\mathrm{N}_{\mathrm{O}^-}-\mathrm{N}_{\mathrm{e},0}\exp\left(\frac{\varphi-\varphi_0}{\mathrm{T}_{\mathrm{e,eV}}}\right)\right]\mathrm{d}\,V+\int_{\mathrm{S_D}}\rho_\Sigma \mathrm{d}\,S=0. \qquad (4)$$

Dielectric interface

As previously mentioned, a surface charge density ρ_Σ can be produced by secondary emission due to a flux of positive ions on the dielectric surface, or by a flux of electrons. In the first case, a secondary emission event is assumed to leave a hole (i.e., a positive charge) on the dielectric surface. Neglecting the diffusion fluxes, the ionic flux toward the dielectric wall depends on the normal component of the electric field E_n (the normal unit vector is assumed to point outward the calculation domain, i.e., toward the dielectric wall). The time variation of the cumulated surface charge density is then described as follows:

$$\frac{\mathrm{d}\rho_\Sigma}{\mathrm{dt}}=e\,\gamma\left(\mu_{\mathrm{N}_2^+}\mathrm{N}_{\mathrm{N}_2^+}+\mu_{\mathrm{O}_2^+}\mathrm{N}_{\mathrm{O}_2^+}\right)\mathrm{E_n},\ \ \mathrm{E_n}>0, \qquad (5)$$

where γ is the secondary emission coefficient for the given dielectric layer material. Conversely, an electron flux toward the dielectric wall is assumed to produce an instantaneous neutralization of holes, if they are present, or a negative charge accumulation otherwise. The following relation is employed in both cases:

$$\frac{\mathrm{d}\rho_\Sigma}{\mathrm{dt}}=e\,\mu_\mathrm{e}\mathrm{N_e}\,\mathrm{E_n},\ \ \mathrm{E_n}<0. \qquad (6)$$

Streamers modelling

Streamers are a fundamental feature in DBDs, as they essentially contribute in producing ionization and charge transfer. However, the typical lifetime of a streamer discharge is extremely short when

compared to the characteristic time of the heavy species. Since the model described in this paper is conceived to treat phenomena evolving with the characteristic time of the heavy species, the formation and the evolution of a streamer cannot be adequately represented. However, a specifically tailored approach has been developed for taking into account the net contribution of streamers to the discharge. The streamer is represented by the series of a non-linear time dependent resistor with two capacitors. The electric current I_e flowing through the streamer section $\mathrm{S_s}$ is defined as the flux of electrons through it, due to the motion impressed by the electric field:

$$\mathrm{I_e} = \int_{\mathrm{S_s}} \mathrm{e\,N_e}\langle \mathrm{v_e}\rangle \cdot \hat{\mathrm{n}}\mathrm{d}S \approx e\mathrm{N_e}\mu_\mathrm{e}\frac{\Delta\varphi}{\mathrm{L_g}}\mathrm{S_s}, \tag{7}$$

where L_g is the length of the streamer (which is considered to be equal to the air gap width) and $\Delta\varphi$ is the voltage across it. A 0.2 $\mathrm{mm^2}$ $\mathrm{S_s}$ section has been taken for the calculations, according to [14].

The electrons number density evolution in time is governed by the following equation:

$$\frac{\mathrm{dN_e}}{\mathrm{dt}} = \alpha\frac{\mathrm{I_e}}{\mathrm{eS_s}}, \tag{8}$$

in which α represent the sum of the first Townsend ionization coefficients for the considered neutral species. Equation (8), coupled with (7), allows one to evaluate the net production of species during a streamer discharge. These results are then used to evaluate the source terms $\Omega_{s,streamer}$ in (1).

Plasma Kinetics

As already stated, the terms Ω_s in (1) describes the number density variation in time due to the plasma kinetics and to the chemical reactions within the discharge. The above mentioned source terms are evaluated at each time step, by solving an independent system of ordinary differential equations

for every node of the computational mesh. The considered elementary processes that have been considered for this work are listed in Tab. 1. The employed reaction rates can be found in [15] or [16], as indicated the right column of Tab. 1. Impact ionization, responsible for the avalanche effect, is not included in Tab. 1; indeed, it has already been taken into account in the streamer model. The characteristics of the proposed model (i.e. the relatively low computational burden) allows to include more complex and accurate descriptions of transport parameters [17] and plasma kinetics [18]. Future development will explore this possibility. Also, other gases will be considered, and atomic gases [19] are especially well suited for an experimental validation of the code.

NUMERICAL MODEL

The problem formulated in the previous section has been solved numerically using a two-dimensional Finite Volume (FV) approach. The discrete balance equation provided by (1) is integrated in time by means of an explicit Euler scheme. In order to grant the numerical stability of the Euler integrator, the time step $\Delta t^{(k)}$ to be employed at the kth iteration is obtained by evaluating the Courant-Friedrichs-Lewy (CFL) condition for each specie with the following expression:

$$\Delta t^{(k)} = K_c \frac{\Delta}{2D_s/\Delta + \mu_s E}, \tag{9}$$

where Δ is the minimum spacing of the adopted cartesian grid, and K_c the adopted Courant coefficient for the presented simulations, i.e., 0.8. After the evaluation of (9) for all the heavy species, the $\Delta t^{(k)}$ to be employed in the drift-diffusion equations is selected as the most restrictive among the obtained results. The CFL stability condition is computed accounting for the convective and diffusive terms of (1). Nevertheless, (1) also contains a source term due to elementary processes, Ω_s, whose analytical expression changes depending on the considered reactions. Hence, the time step obtained with the CFL condition doesn't account for the source terms, that therefore must be computed separately. The

variation of the number densities during the time step $\Delta t^{(k)}$ is calculated by employing the semi-implicit approach described in [9], yielding the following linearized expression for the local number density increment with respect to a generic time-instant k:

$$\{\Delta N_s\} = \left\{\Omega_s^{(k)}\right\} \Delta t\left[I_d - 1/2\left[J^{(k)}\right]\Delta t\right]^{-1}. \quad (10)$$

In (10), $\{\Delta N_s\}$ is the array of the local number density increments relative to each species in the time step Δt, whereas the array $\left\{\Omega_s^{(k)}\right\}$ contains the source terms evaluated at time instant k. $[I_d]$ is the identity matrix, and $\left[J^{(k)}\right]$ is the local jacobian matrix of the source terms. At the generic time instant k, the Euclidean norm of the matrix $[1/2\, J^{(k)}\Delta t]$ is checked using the Δt^k yielded by the CFL condition. The required stability condition is expressed as:

$$\left\|1/2\left[J^{(k)}\right]\Delta t\right\| < \beta_k,\ \beta_k = 0.25. \quad (11)$$

If condition (11) is not satisfied, the semi-implicit time integration is split in the required number of sub steps to cover the time step $\Delta t^{(k)}$ without losses of accuracy. At each time step, the nonlinear Poisson equation (3) is discretized using a finite volume approach. The resulting nonlinear algebraic system is solved by means of a Newton-Raphson algorithm. The solution obtained yields the distribution of the electric potential as a function of the reference potential φ_0. This quantity is adjusted to meet the neutrality of the total electric charge constraint (4) by means of an iterative solver running externally to the Newton-Raphson solver. In carrying out this task, the bisector method showed good reliability and robustness. The Meek's criterion [6] is used to check whether the conditions for the streamers formation are verified, and the ionized species produced are added.

RESULTS AND DISCUSSION

The numerical model presented in this paper has been employed to simulate the main plasma dynamics taking place in a 0.8 mm x 4.0 mm parallel electrodes DBD reactor with a 0.8 mm airgap. The four sides of the domain will be referred hereon as South (S), East (E), North (N) and West (W), with the external sinusoidal voltage applied between the N and S sides, as sketched in Fig. 1. The calculation domain has been discretized with a structured, non-uniform, bi-dimensional grid consisting of 111 nodes on the N-S direction and 41 nodes on the E-W direction. In order to adequately discretize the sheath region toward the electrodes, the grid has been refined approaching the edges of the domain for both the N-S and E-W directions. In particular, the spacing in the N-S direction ranges from a minimum value of 4 μm at the border to a maximum of 12 μm at the midpoint of the gap. The two electrodes are assumed to be separated from the air gap by a 0.1 mm thick layer of teflon ($\varepsilon_d = 2.1$, $\gamma = 0.1$). A sinusoidal voltage of amplitude 4.8 kV and frequency 50 kHz has been enforced between the two electrodes. The simulation has been performed assuming atmospheric pressure air; hence, the number densities of N_2 and O_2 have been set to 1.88 10^{25} m^{-3} and 0.63 10^{25} m^{-3}, respectively.

The temperatures of the electrons and the heavy species have been set to 20000 K and 400 K respectively. Ion mobilities are taken from [6], while the diffusion coefficients are evaluated using the Einstein relation, i.e., $D_s = \mu_s/(k_b T)$.

Figure 2.a shows the total positive electric charge deposited on the dielectric surfaces due to secondary emission as a function of time, whereas Fig. 2.b depicts the external voltage applied between the electrodes V_{ext} and the voltage across the gap V_{gap}. The difference between the two curves is caused by the voltage drop across the dielectric barrier and to the surface electric charge.

It is worth highlighting that V_{gap} (pink, dashed line in Fig. 2.b) is the potential difference to which the charged species are subjected. Notably, V_{gap} drops to almost 0V after roughly 2 μs in the first cycle. This effect is produced by the surface charge density accumulated on the dielectric layers of the DBD reactor due to a combination of drift and diffusion towards the walls. Figure Fig. 2.c shows

the evolution of the time step length employed for the explicit time integration of the drift and diffusion equations throughout the simulation. As one can see, the shortest steps length are obtained when the deposited surface charge is low. Indeed, the absence of the surface charge screening effect leads to higher electric field magnitudes in the gap.

Some details of the calculated distributions of the charged species are shown for two significant instants of the simulation τ_1 and τ_2, with $\tau_1 = 17$ μs and at $\tau_2 = 20$ μs.

In τ_1 the applied voltage to the electrodes is nearly 2.5 kV. As one can see by looking at Fig. 2, at this stage the deposited charge on the dielectric S has just reached zero, and the charge deposited on the dielectric N is starting to raise. Indeed, a peak of positive charge can be observed towards the edge N in Fig. 2(a). This charge has been drifting from the edge S since the voltage inversion at 15 μs. Still, a rather high number density of N_{2^+} can be observed near S. This is due to the high electrons number density distribution of Fig. 3(b) near S, that triggers the production of positively charged heavy species via ionization.

When the time instant τ_2 is reached, the externally applied voltage is maximum, but the gap is subjected to just 80 V, as can be observed in Fig.3(a). This effect is due to the positive charge deposited on the dielectric N. Finally, figure 4(b) shows the ozone produced since the beginning of the simulation.

CONCLUSIONS

In this work, a 2D multi-stage model for the simulation of the main physical processes taking place in a DBD in atmospheric pressure air has been presented. The proposed numerical strategy limits the explicit time integration of the drift and diffusion equations to the heavy ionic and neutral species, aiming to limit the required computational times. For the same reason, a simplified model has been introduced to represent the macroscopic effects of the streamer discharges taking place in the plasma bulk. The developed model has been applied to the simulation of a DBD volumetric reactor, and the obtained results are compatible with the expected physical behaviour of both the electrons and heavy

species. Although only the main charge deposition mechanisms have been included in the model, the results for the accumulated surface charge on the dielectric layers appear to be realistic. In addition, the present work highlights the importance of the macroscopic effects exerted the accumulated surface charge on the plasma dynamics for this kind of configurations. Future work will be devoted to include the contribution of exited states, as well as more detailed physical processes for the charge deposition mechanisms.

REFERENCES

[1] E. Moreau, "Airflow control by non-thermal plasma actuators," *J. Phys. D. Appl. Phys.*, vol. 40, no. 3, pp. 605–636, Feb. 2007.

[2] G. Neretti, A. Cristofolini, C. A. Borghi, A. Gurioli, and R. Pertile, "Experimental results in DBD plasma actuators for air flow control," *IEEE Trans. Plasma Sci.*, vol. 40, no. 6 PART 2, pp. 1678–1687, 2012.

[3] J. Wang, Y. Li, Z. An, C. Wang, and S. Hou, "Shock wave control by dielectric barrier discharge and arc discharge in a Mach 2.2 cold supersonic airflow," *Int. J. Appl. Electromagn. Mech.*, vol. 33, no. 3–4, pp. 1391–1396, 2010.

[4] S. Roy, P. Zhao, A. DasGupta, and J. Soni, "Dielectric barrier discharge actuator for vehicle drag reduction at highway speeds," *AIP Adv.*, vol. 6, no. 2, Feb. 2016.

[5] D. Ashpis, D. T.-I. J. of T. & Jet, and undefined 2019, "Dielectric Barrier Discharge (DBD) Plasma Actuators for Flow Control in Turbine Engines: Simulation of Flight Conditions in the Laboratory by Density Matching," *degruyter.com*.

[6] A. Fridman, *Plasma chemistry*. Cambridge university press, 2008.

[7] R. Laurita, D. Barbieri, M. Gherardi, V. Colombo, and P. Lukes, "Chemical analysis of reactive species and antimicrobial activity of water treated by nanosecond pulsed DBD air plasma," *Clin. Plasma Med.*, vol. 3, no. 2, pp. 53–61, 2015.

[8] H. Shintani, A. Sakudo, P. Burke, and G. McDonnell, "Gas plasma sterilization of microorganisms and mechanisms of action," *Exp. Ther. Med.*, vol. 1, no. 5, pp. 731–738, 2010.

[9] A. Cristofolini and A. Popoli, "A multi-stage approach for DBD modelling," in *Journal of Physics: Conference Series*, 2019, vol. 1243, no. 1, p. 12012.

[10] A. V Likhanskii, M. N. Shneider, S. O. Macheret, and R. B. Miles, "Modeling of dielectric barrier discharge plasma actuator in air," *J. Appl. Phys.*, vol. 103, no. 5, p. 53305, 2008.

[11] J. S. Shang and P. G. Huang, "Modeling of ac dielectric barrier discharge," *J. Appl. Phys.*, vol. 107, no. 11, p. 113302, Jun. 2010.

[12] S. Yamamoto and K. Fukagata, “Numerical simulation of a plasma actuator based on ion transport,” *J. Appl. Phys.*, vol. 113, no. 24, p. 243302, 2013.

[13] J. P. Boeuf, Y. Lagmich, T. Unfer, T. Callegari, and L. C. Pitchford, “Electrohydrodynamic force in dielectric barrier discharge plasma actuators,” 2007.

[14] G. Wormeester, S. Pancheshnyi, A. Luque, S. Nijdam, and U. Ebert, “Probing photo-ionization: simulations of positive streamers in varying N2: O2-mixtures,” *J. Phys. D. Appl. Phys.*, vol. 43, no. 50, p. 505201, 2010.

[15] B. Parent, S. O. Macheret, and M. N. Shneider, “Electron and ion transport equations in computational weakly-ionized plasmadynamics,” *J. Comput. Phys.*, vol. 259, no. April 2018, pp. 51–69, 2014.

[16] I. A. Kossyi, A. Y. Kostinsky, A. A. Matveyev, and V. P. Silakov, “Kinetic scheme of the non-equilibrium discharge in nitrogen-oxygen mixtures,” *Plasma Sources Sci. Technol.*, vol. 1, no. 3, p. 207, 1992.

[17] A. Laricchiuta *et al.*, “Classical transport collision integrals for a Lennard-Jones like phenomenological model potential,” *Chem. Phys. Lett.*, vol. 445, no. 4–6, pp. 133–139, 2007.

[18] G. Colonna, G. D’Ammando, and L. D. Pietanza, “The role of molecular vibration in nanosecond repetitively pulsed discharges and in DBDs in hydrogen plasmas,” *Plasma Sources Sci. Technol.*, vol. 25, no. 5, p. 54001, 2016.

[19] G. Capriati, G. Colonna, C. Gorse, and M. Capitelli, “A parametric study of electron energy distribution functions and rate and transport coefficients in nonequilibrium helium plasmas,” *Plasma Chem. plasma Process.*, vol. 12, no. 3, pp. 237–260, 1992.

Table 1: chemical reactions included in the model.

Ionizations	$N_2 + e$	$\rightarrow$	$N_2^+ + e^- + e^-$	[15]
	$O_2 + e$	$\rightarrow$	$O_2^+ + e^- + e^-$	[15]
Recombinations	$N_2^+ + e^-$	$\rightarrow$	N_2	[15]
	$O_2^+ + e^-$	$\rightarrow$	O_2	[15]
	$N_2^+ + O_2^-$	$\rightarrow$	$N_2 + O_2$	[15]
	$O_2^+ + O_2^-$	$\rightarrow$	$O_2 + O_2$	[15]
	$N_2 + N_2^+ + O_2^-$	$\rightarrow$	$N_2 + N_2 + O_2$	[15]
	$N_2 + O_2^+ + O_2^-$	$\rightarrow$	$N_2 + O_2 + O_2$	[15]
	$O_2 + N_2^+ + O_2^-$	$\rightarrow$	$N_2 + O_2 + O_2$	[15]
	$O_2 + O_2^+ + O_2^-$	$\rightarrow$	$O_2 + O_2 + O_2$	[15]
Attachment	$N_2 + O_2 + e^-$	$\rightarrow$	$N_2 + O_2^-$	[15]
	$O_2 + O_2 + e^-$	$\rightarrow$	$O_2 + O_2^-$	[15]
	$O_2 + O + e^-$	$\rightarrow$	$O_2 + O^-$	[15]
	$O_3 + e^-$	$\rightarrow$	$O_2 + O^-$	[16]
	$O_3 + e^-$	$\rightarrow$	$O_2^- + O$	[16]
Detachment	$O_2 + O_2^-$	$\rightarrow$	$O_2 + O_2 + e^-$	[15]
	$O_2 + O^-$	$\rightarrow$	$O_3 + e^-$	[16]
Dissociation	$O_2 + e^-$	$\rightarrow$	$O + O + e^-$	[16]
	$O_3 + e^-$	$\rightarrow$	$O_2 + O + e^-$	[16]
O_3 formation	$O + O_2 + N_2$	$\rightarrow$	$O_3 + N_2$	[16]
	$O + O_2 + O_2$	$\rightarrow$	$O_3 + O_2$	[16]

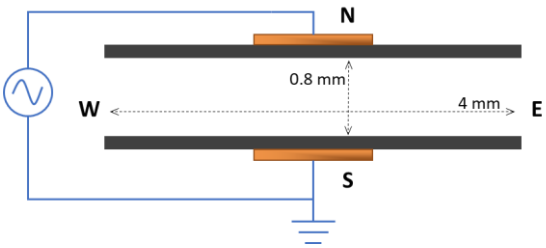

Figure 1: Sketch of the considered parallel plate DBD device.

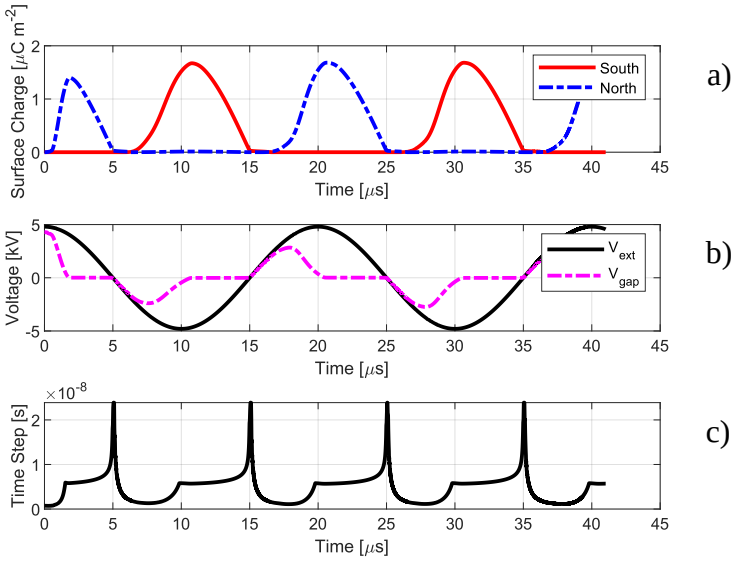

Figure 2. a) deposited surface charge, b) applied voltage and c) time step vs time.

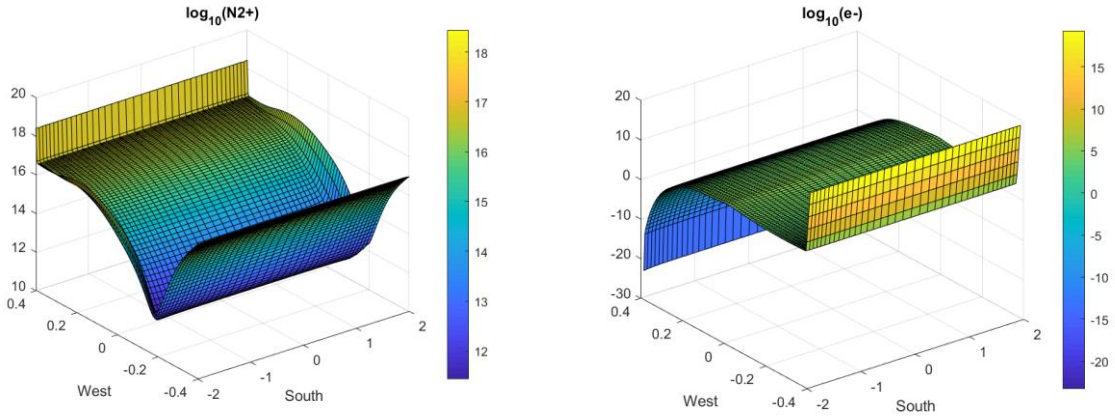

a) b)

Figure 3. Positive nitrogen ions a) and electron b) number density distribution at $\tau_1 = 17$ μs.

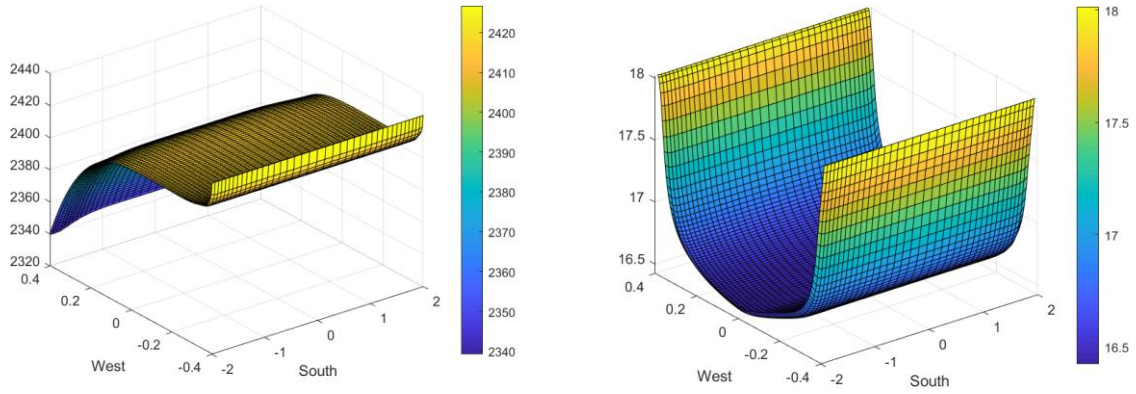

a) b)

Figure 4. Electric potential a) and ozone b) number density distribution at $\tau_2 = 20$ μs.